

Studies on dim-8 EFT limit setting in p-p collisions at $\sqrt{s} = 13$ TeV for the EWK production of ZZjj in the four-lepton channel

HEP 2021 - 38th Conference on Recent Developments in High Energy Physics and Cosmology
16-19 June 2021, Thessaloniki, Greece.

Alexandros Marantis

Hellenic Open University



Outline

Observation of EWK production of ZZjj at the ATLAS experiment

- EWK – QCD Tree-Level feynman diagrams
- Phase-space definition
- Observation
- Measurement of fiducial cross-section

(see detailed presentation on an overview of the VBS ZZjj analysis of Run-II data at the ATLAS experiment, by Ioannis Maznas)

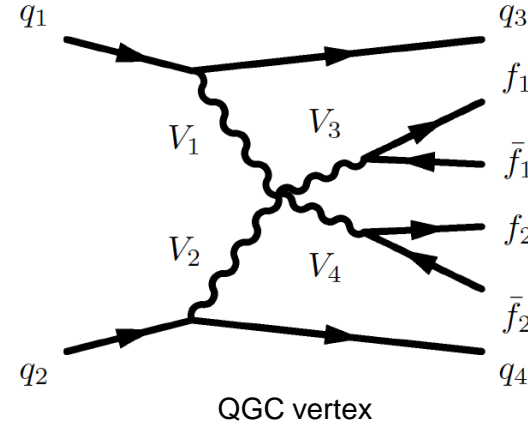
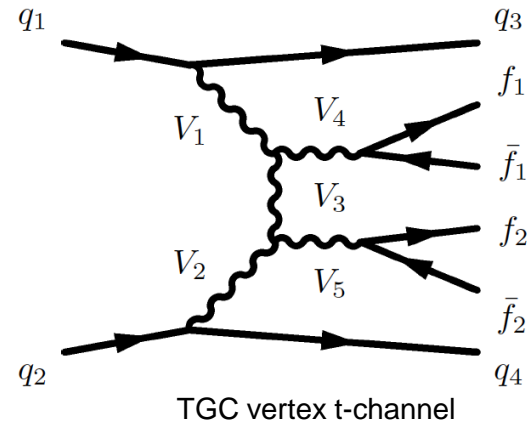
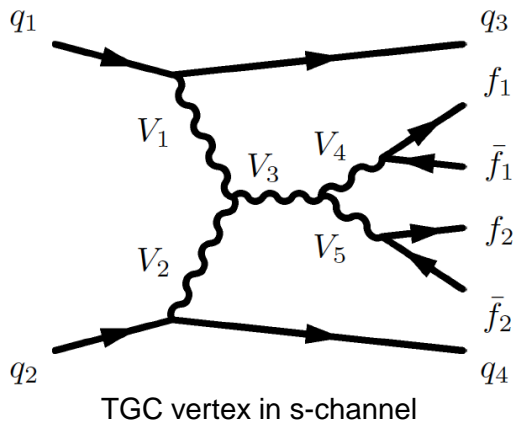
Anomalous Quartic Gauge Couplings (aQGC)

- Decomposition method
- Choice of the discriminant variable
- Sensitivity of QGC operators
- Limit setting strategy

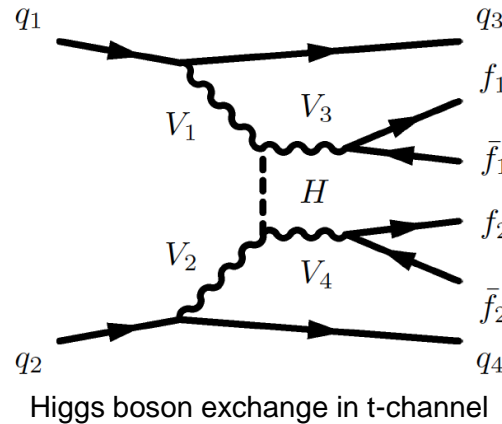
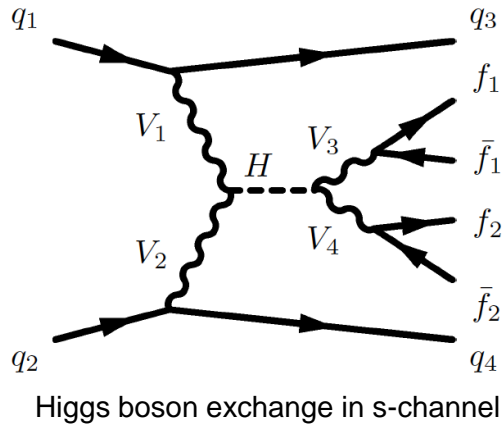
Electroweak (EWK) signal

Measurement of Vector Boson pair production provides an excellent test of the ElectroWeak Symmetry Breaking (EWKSB) sector of the Standard Model (SM).

The VBS topology consists of two high energy jets in the back and forward regions, with two vector bosons.



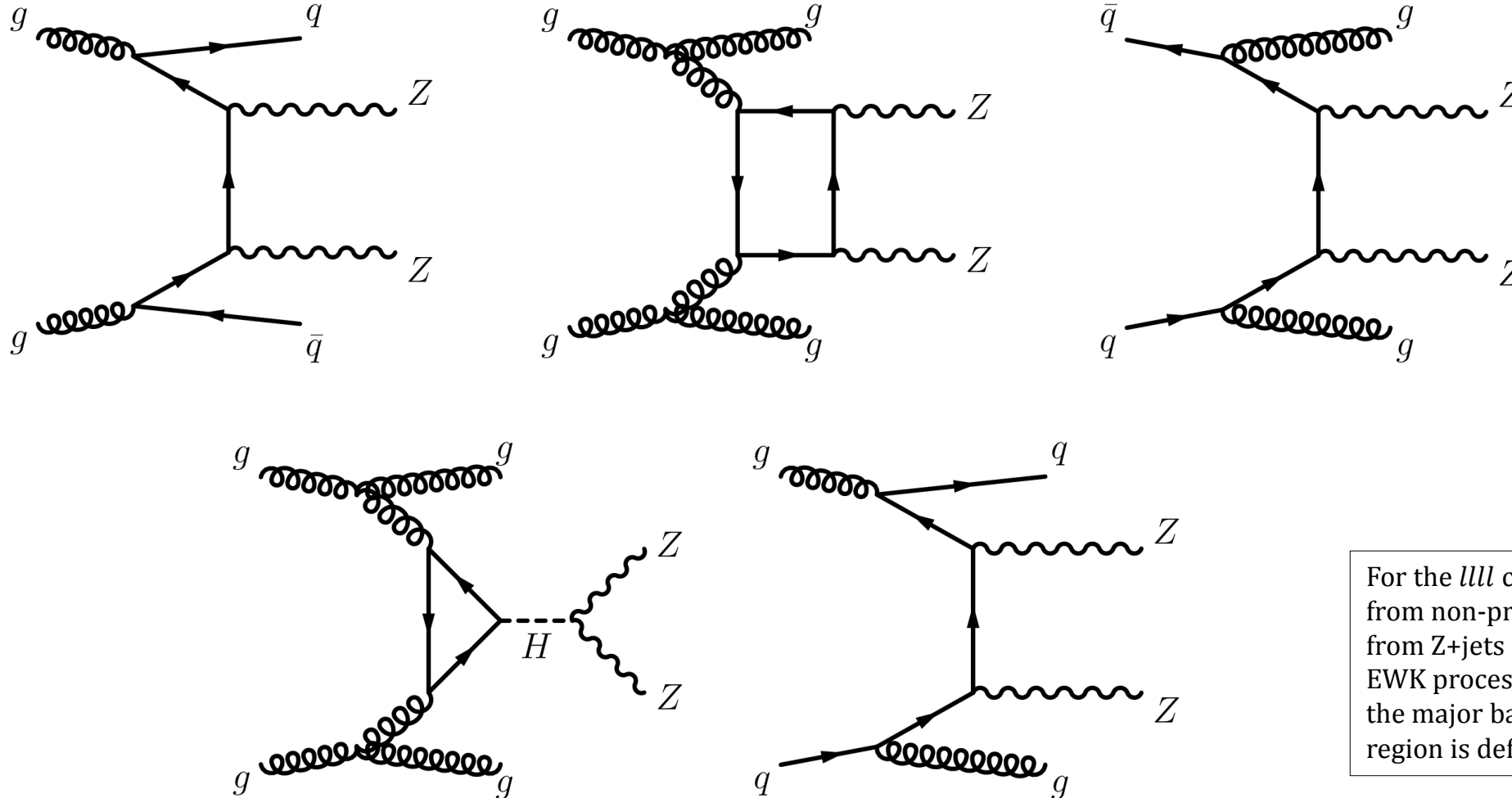
- Quartic Gauge Couplings (QGCs)
- Only charged QGCs allowed at SM tree-level ($WWWW$, $WWZZ$, $WWZ\gamma$, $WW\gamma\gamma$)
 - Constraint on anomalous QGCs



- Crucial channel for Higgs discovery
- A precision measurement helps in Higgs property measurement
 - Search of high mass Higgs bosons
 - Proves the SM Higgs mechanism

Quantum Chromodynamics (QCD) background

The main background processes for the $ZZ \rightarrow jjllll$ VBS channels are the QCD background and the fake (misidentified leptons) background.



+

Fake background:

- $Z + jets$
- $t\bar{t}$

For the $llll$ channel, there are small contributions from non-prompt backgrounds, from fake leptons from Z +jets and top processes. When looking at the EWK processes alone, the QCD component becomes the major background and a QCD-enriched control region is defined to constrain the contribution.

Total and Fiducial Phase Space

Total phase space and Fiducial phase space are defined for the cross-section measurement in $llll$ channel.

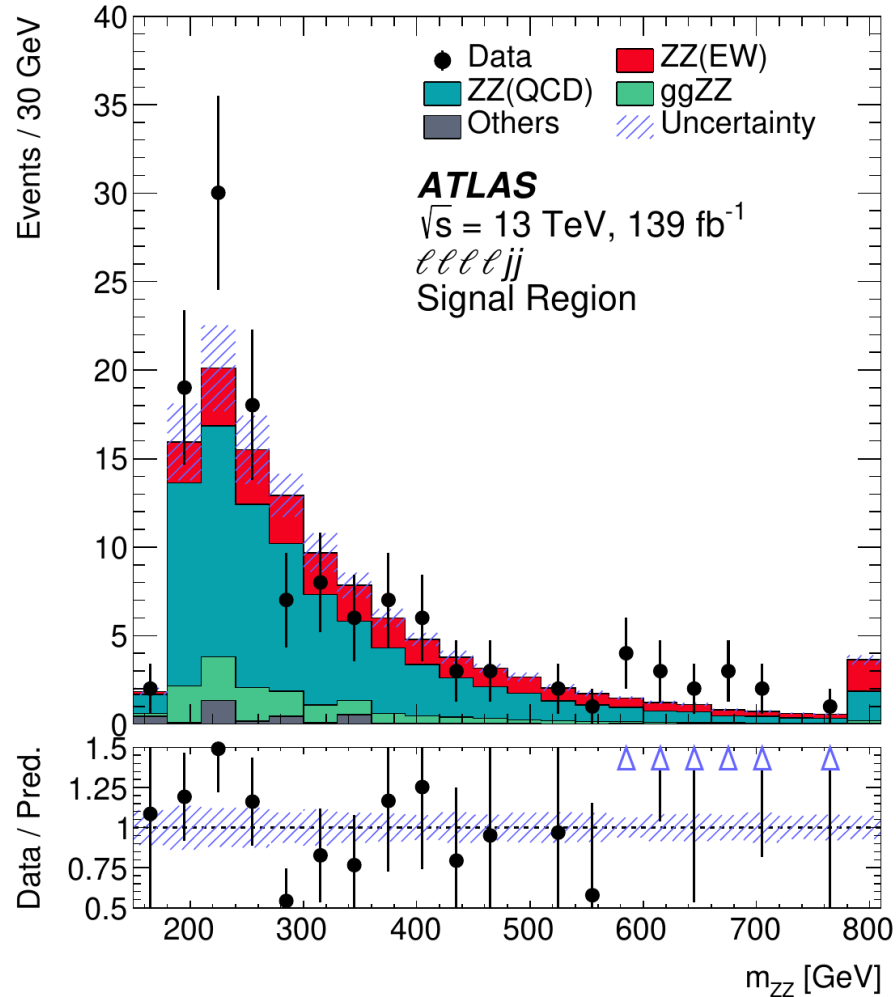
Total PS definition

- $p_T^l > 5 \text{ GeV}$
- $|\eta^l| < 2.7$
- *ZZ candidates, minimizing $|m_{Z_1} - m_{Z_p}| + |m_{Z_2} - m_{Z_p}|$.*
The one SFOS pair with dilepton mass closest to Z mass is labelled as Z_1
- $66 < m_Z < 116 \text{ GeV}$
- $m_{l+l-} > 10 \text{ GeV}$ for SFOS dilepton pairs
- *At least two AntiKt4 truth jets with $p_T > 20 \text{ GeV}$ and $|\eta| < 5$*
- *Leading jets from detector A and C side: $\eta^{j1} \times \eta^{j2} < 0$*
- $m_{jj} > 200 \text{ GeV}$

Fiducial PS definition (in addition to Total PS selections)

- $|\eta^e| < 2.47, |\eta^\mu| < 2.7$
- $p_T^l > 20, 20, 10, 7 \text{ GeV}$ for the leading, sub-leading, third and fourth lepton
- $\Delta R(l, l) > 0.2$
- $p_T^j > 30 (40) \text{ GeV}$ for jets with $|\eta^j| < 2.4 (4.5)$
- $|\Delta\eta(jj)| > 2$

Observation & Measurement summary



Process	$l\bar{l}l\bar{l}jj$
EW $ZZjj$	20.6 ± 2.5
QCD $ZZjj$	77 ± 25
QCD $ggZZjj$	13.1 ± 4.4
Non-resonant- $l\bar{l}$	–
WZ	–
Others	3.2 ± 2.1
Total	114 ± 26
Data	127

Observed data and expected event yields in 139 fb^{-1} of data in the $4lj$ signal region. All the minor backgrounds are summed together as ‘Others’. Uncertainties in the predictions include both the statistical and systematic components.

Measured and predicted fiducial cross-section in the $4lj$ channel for the inclusive $ZZjj$ processes.

	Measured fiducial σ [fb]	Predicted fiducial σ [fb]
$l\bar{l}l\bar{l}jj$	$1.27 \pm 0.12(\text{stat}) \pm 0.02(\text{theo}) \pm 0.07(\text{exp}) \pm 0.01(\text{bkg}) \pm 0.03(\text{lumi})$	$1.14 \pm 0.04(\text{stat}) \pm 0.20(\text{theo})$

Anomalous Quartic Gauge Couplings

- Neutral couplings $ZZZZ, ZZZ\gamma, ZZ\gamma\gamma, Z\gamma\gamma\gamma$ are forbidden in the Standard Model
- Effects increase with $\sqrt{\hat{s}}$
- Presence of aQGCs lead to enhancement of the cross section and modification of event kinematics in high p_T , high E_T or high mass regions
 - study of variables that carry system's energy (p_T, m_{ZZ})
- Shape difference between SM and aQGC MC kinematic distributions
- Common choice: effective field theory (EFT) with higher order dimensions operators
- Effective Lagrangian Approach

$$\mathcal{L}_{EFT} = \mathcal{L}_{SM} + \sum_{d>4} \sum_i \frac{c_i^{(d)}}{\Lambda^{d-4}} \mathcal{O}_i^{(d)}$$

- Set of dim-8 operators affecting quartic boson vertices:

	WWWW	WWZZ	ZZZZ	WWAZ	WWAA	ZZZA	ZZAA	ZAAA	AAAA
$\mathcal{O}_{S,0}, \mathcal{O}_{S,1}$	X	X	X						
$\mathcal{O}_{M,0}, \mathcal{O}_{M,1}, \mathcal{O}_{M,6}, \mathcal{O}_{M,7}$	X	X	X	X	X	X	X		
$\mathcal{O}_{M,2}, \mathcal{O}_{M,3}, \mathcal{O}_{M,4}, \mathcal{O}_{M,5}$		X	X	X	X	X	X		
$\mathcal{O}_{T,0}, \mathcal{O}_{T,1}, \mathcal{O}_{T,2}$	X	X	X	X	X	X	X	X	X
$\mathcal{O}_{T,5}, \mathcal{O}_{T,6}, \mathcal{O}_{T,7}$		X	X	X	X	X	X	X	X
$\mathcal{O}_{T,8}, \mathcal{O}_{T,9}$			X			X	X	X	X

Overview of EFT studies

- Use of MadGraph5 v2.6.1 @LO with Éboli & Gonzalez-Garcia UFO model for **generation** of $pp \rightarrow ZZjj \rightarrow l^+l^-l^+l^-jj$ samples with the **decomposition method**
- Determine the most **sensitive discriminant** (kinematic variable) to use for the EFT studies
- Create a grid of aQGC points for **checking the sensitivity** of the operators O_M, O_S and O_T
- aQGC limit extraction strategy: Construction of the **likelihood function** with the aQGC parameters

$$L(N_i^{obs}; N_i^{exp}, f_T) = \prod_{i=1}^{N_{bin}} P(N_i^{obs}, N_i^{exp}) = \prod_{i=1}^{N_{bin}} \frac{e^{-N_i^{exp}} (N_i^{exp})^{N_i^{obs}}}{(N_i^{obs})!}$$

Decomposition method of QGCs

EFT dim-8 predictions can be generated in independent samples including the EFT components. The total EFT amplitude can be expressed as:

$$\left| A_{SM} + \sum_i c_i \cdot A_i \right|^2 = |A_{SM}|^2 + \sum_i c_i \cdot 2 \operatorname{Re}(A_{SM}^* \cdot A_i) + \sum_i c_i^2 \cdot |A_i|^2 + \sum_{i,j, i \neq j} c_i c_j \cdot \operatorname{Re}(A_i^* \cdot A_j)$$

Total EFT amplitude

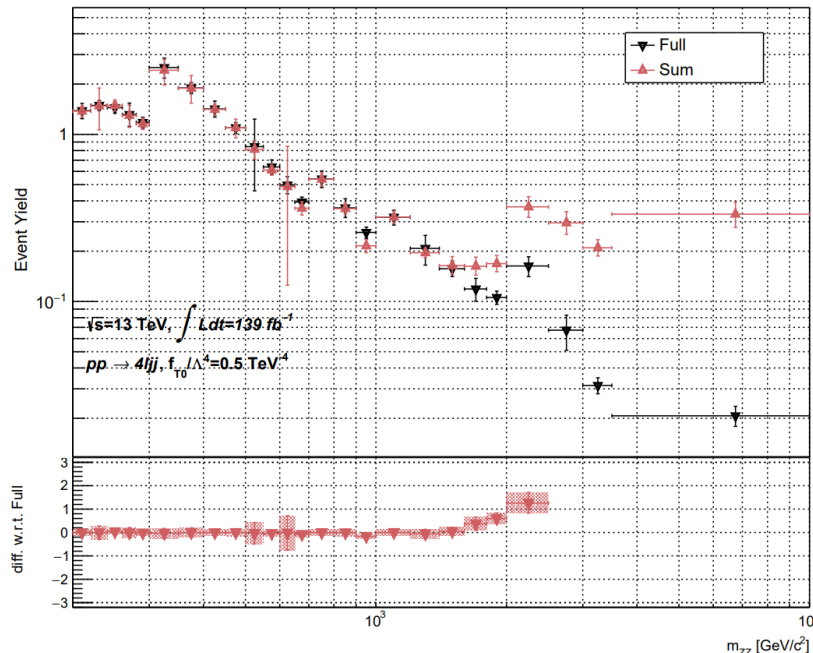
Standard Model

**Interference of SM-aQGC
(linear term)**

**Pure QGC contribution
(quadratic term)**

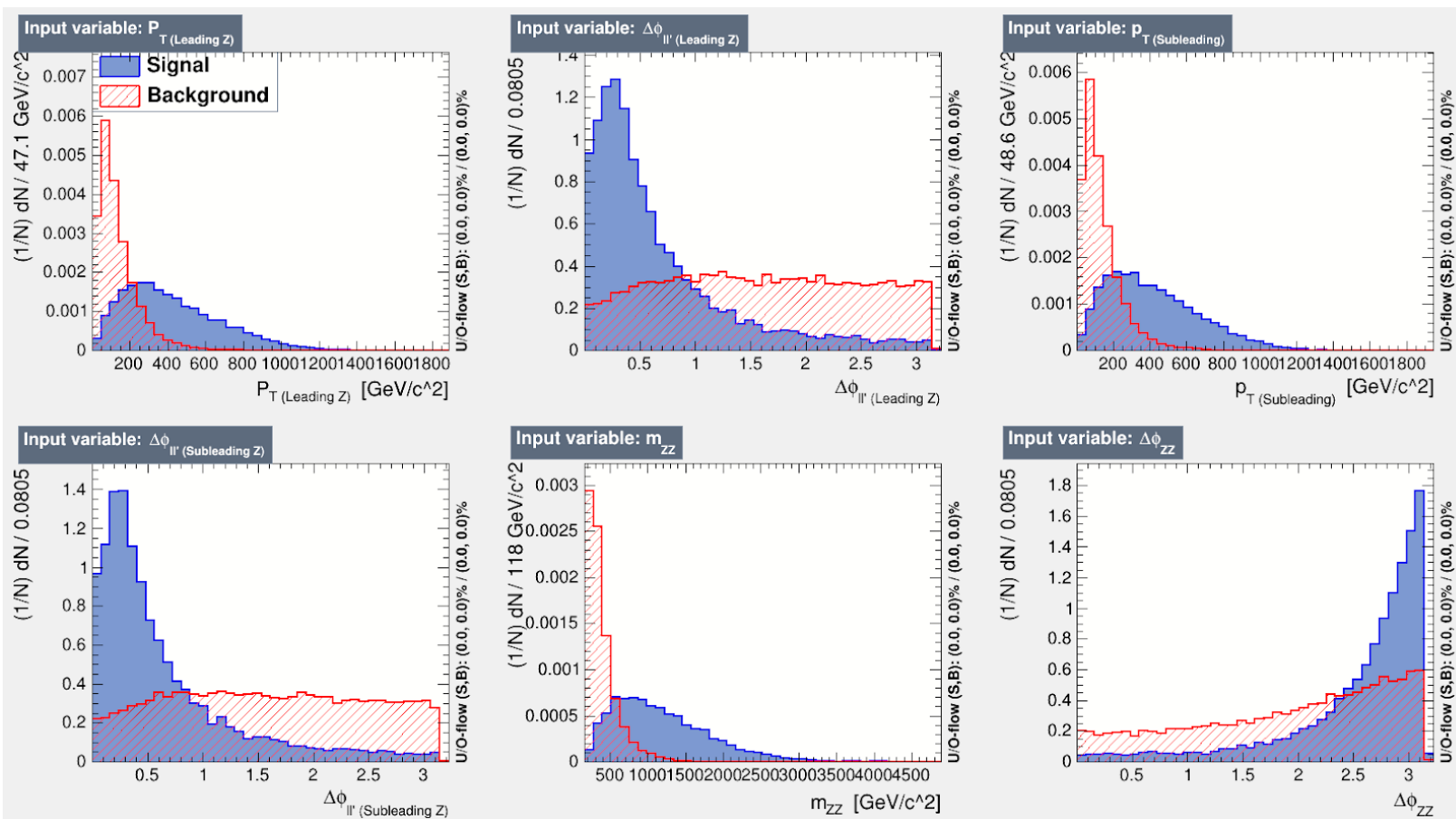
**Interference between QGC operators
(cross terms)**

Minor differences between the samples generated with the total EFT versus the sum of the EFT components.



Discriminant variable selection

- BDT studies, point m_{4l} (in $pp \rightarrow 4ljj$) or m_{ZZ} (in $pp \rightarrow ZZ \rightarrow 4ljj$) as the most sensitive discriminant for the QGC identification
 - Signal: pure QGC sample ($f_{T0}/\Lambda^4 = 0.7 \text{ TeV}^{-4}$) Background: SM EWK sample
 - Input variables used: $p_T^{\text{leading } Z}$, $p_T^{\text{sub-leading } Z}$, m_{ZZ} , $|\Delta\eta_{jj}|$, $|\Delta\eta_{ZZ}|$, $|\Delta\phi_{ll}|$, $|\Delta\phi_{ZZ}|$, p_T^{lepton} , ...



Rank	Variable	Variable Importance
1	ZZ.M	2.084e-01
2	ZZ.dPhiZZ	1.627e-01
3	leadingZ.dPhill	1.593e-01
4	subleadingZ.dPhill	1.591e-01
5	leadingZ.pt	1.560e-01
6	subleadingZ.pt	1.545e-01

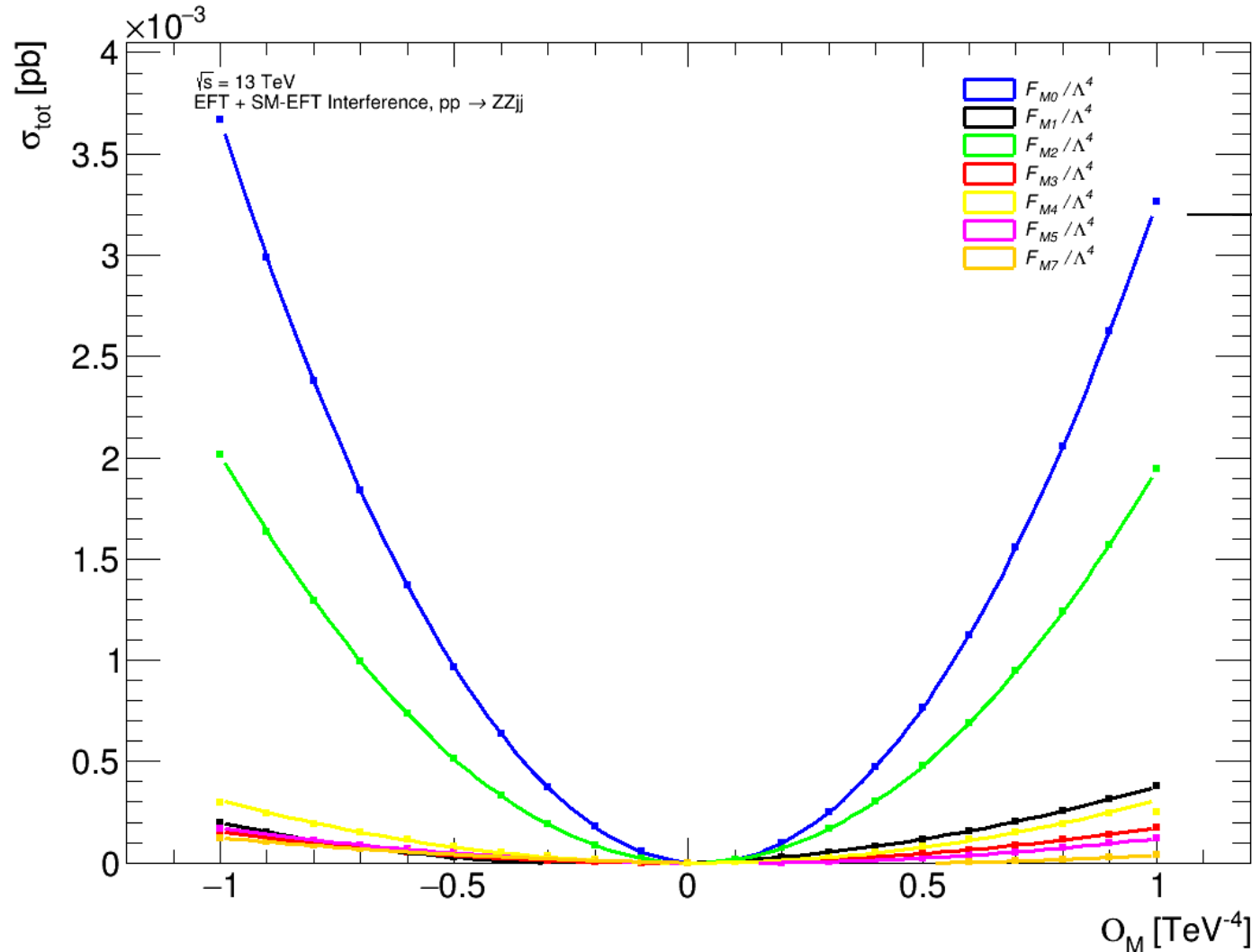
Rank	Variable	Variable Importance
1	ZZ.M	2.255e-01
2	ZZ.dPhiZZ	1.601e-01
3	subleadingZ.dPhill	1.590e-01
4	leadingZ.dPhill	1.585e-01
5	leadingZ.pt	1.513e-01
6	subleadingZ.pt	1.456e-01

Rank	Variable	Variable Importance
1	ZZ.M	1.928e-01
2	ZZ.dPhiZZ	1.812e-01
3	subleadingZ.dPhill	1.743e-01
4	leadingZ.dPhill	1.742e-01
5	subleadingZ.pt	1.425e-01
6	leadingZ.pt	1.349e-01

Sensitivity of QGC operators

$$\mathcal{L}_{EFT} = \mathcal{L}_{SM} + \sum_{j=0,1} \frac{f_{M,j}}{\Lambda^4} \mathcal{O}_{M,j} + \sum_{j=0,1} \frac{f_{S,j}}{\Lambda^4} \mathcal{O}_{S,j} + \sum_{j=0,1} \frac{f_{T,j}}{\Lambda^4} \mathcal{O}_{T,j}$$

Parameter λ (TeV^{-4})	Quadratic function with SM=0 (pb)
F_{M0}/Λ^4	$\sigma(\lambda) = -2.022 \cdot 10^{-4} \cdot \lambda + 3.464 \cdot 10^{-3} \cdot \lambda^2$
F_{M1}/Λ^4	$\sigma(\lambda) = 8.939 \cdot 10^{-5} \cdot \lambda + 2.872 \cdot 10^{-4} \cdot \lambda^2$
F_{M2}/Λ^4	$\sigma(\lambda) = -3.569 \cdot 10^{-5} \cdot \lambda + 1.980 \cdot 10^{-3} \cdot \lambda^2$
F_{M3}/Λ^4	$\sigma(\lambda) = 9.496 \cdot 10^{-6} \cdot \lambda + 1.641 \cdot 10^{-4} \cdot \lambda^2$
F_{M4}/Λ^4	$\sigma(\lambda) = -2.280 \cdot 10^{-5} \cdot \lambda + 2.741 \cdot 10^{-4} \cdot \lambda^2$
F_{M5}/Λ^4	$\sigma(\lambda) = -2.452 \cdot 10^{-5} \cdot \lambda + 1.443 \cdot 10^{-4} \cdot \lambda^2$
F_{M7}/Λ^4	$\sigma(\lambda) = -4.305 \cdot 10^{-5} \cdot \lambda + 7.934 \cdot 10^{-5} \cdot \lambda^2$

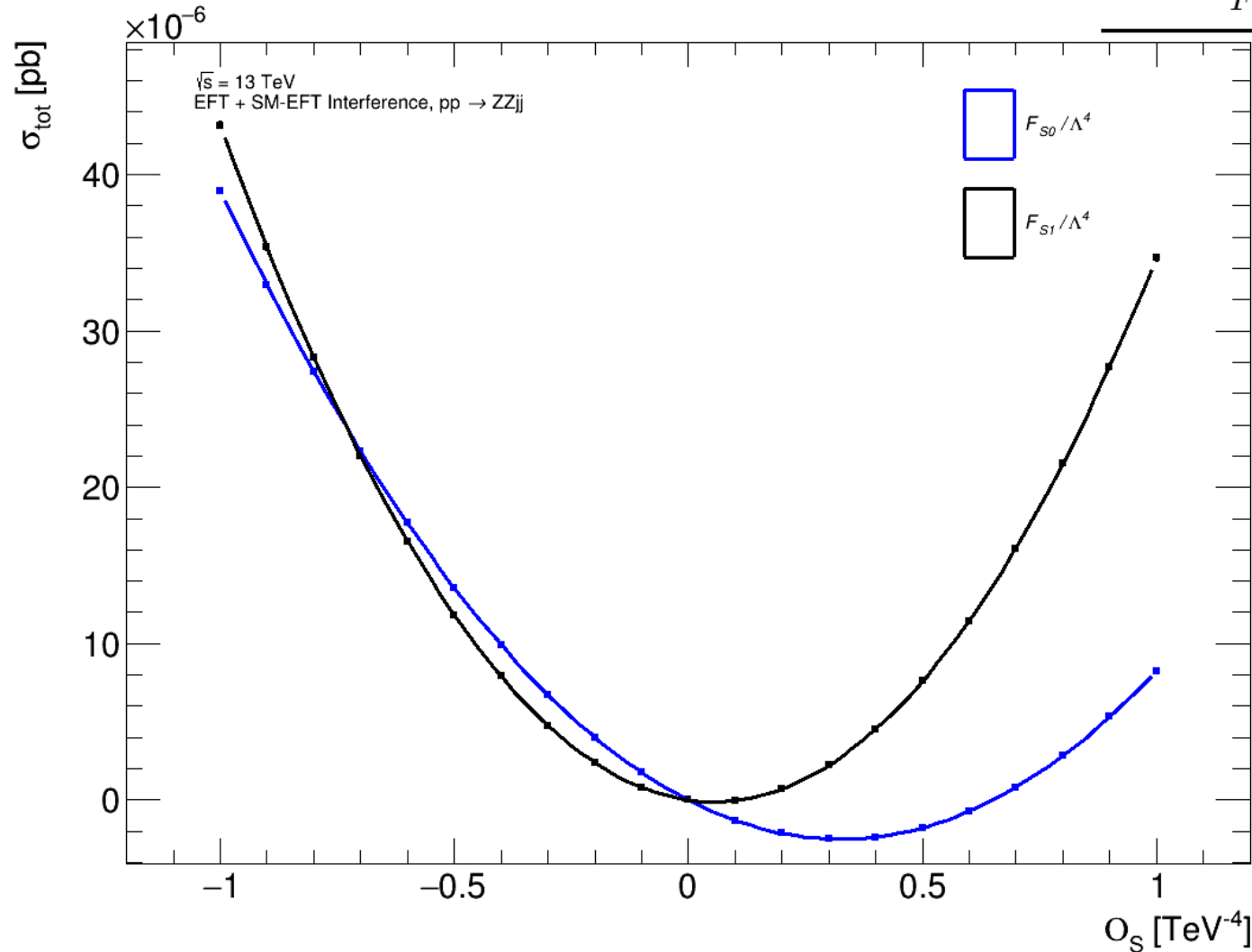


- $pp \rightarrow ZZjj$ samples
- No $Z \rightarrow ll$ applied
- No fiducial cuts applied
- No SM amplitudes includes
 - only linear and quadratic terms

Sensitivity of QGC operators

$$\mathcal{L}_{EFT} = \mathcal{L}_{SM} + \sum_{j=0,1} \frac{f_{M,j}}{\Lambda^4} \mathcal{O}_{M,j} + \sum_{j=0,1} \frac{f_{S,j}}{\Lambda^4} \mathcal{O}_{S,j} + \sum_{j=0,1} \frac{f_{T,j}}{\Lambda^4} \mathcal{O}_{T,j}$$

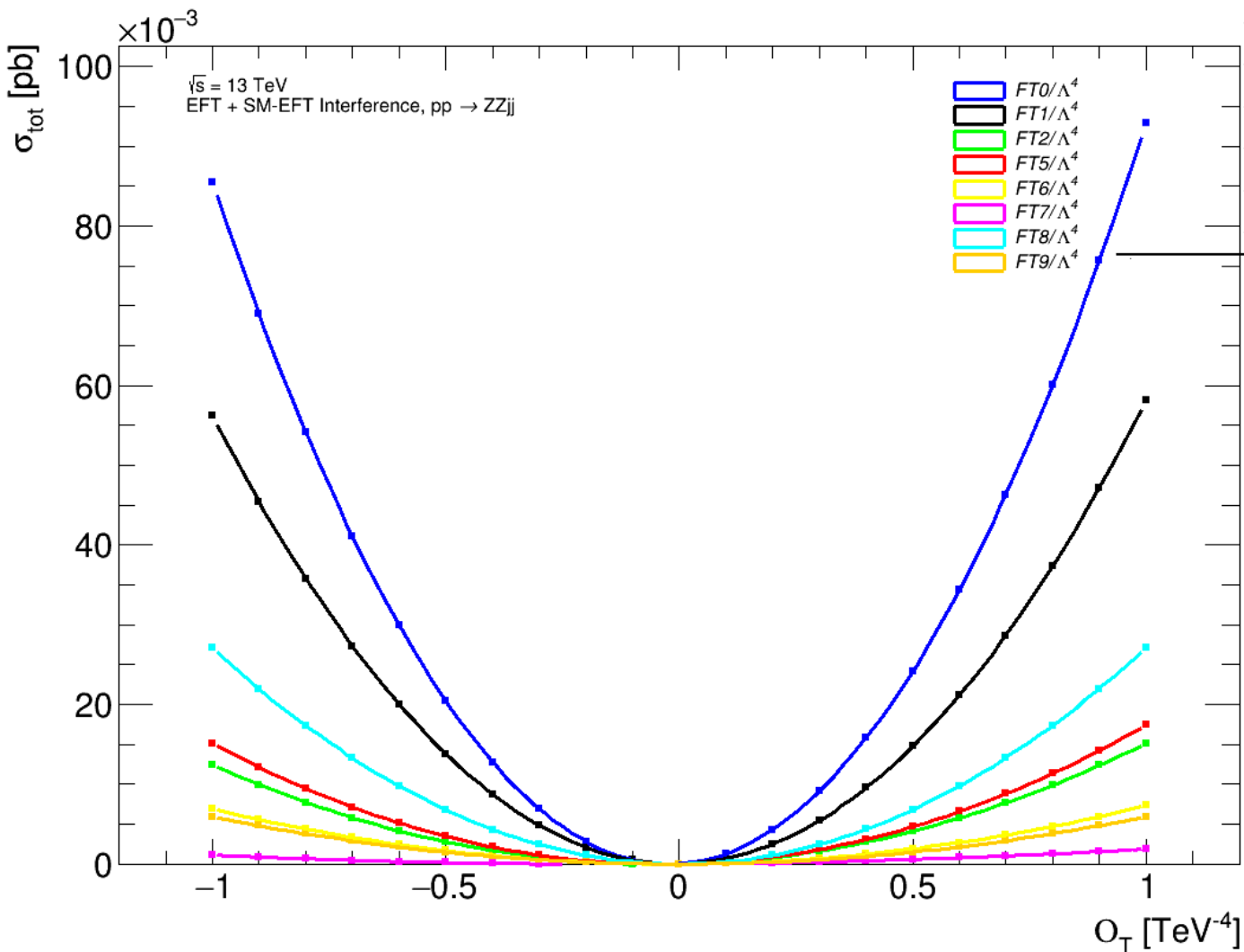
Parameter λ (TeV^{-4})	Quadratic function with SM=0 (pb)
F_{S0}/Λ^4	$\sigma(\lambda) = -1.534 \cdot 10^{-5} \cdot \lambda + 2.362 \cdot 10^{-5} \cdot \lambda^2$
F_{S1}/Λ^4	$\sigma(\lambda) = -4.234 \cdot 10^{-6} \cdot \lambda + 3.890 \cdot 10^{-5} \cdot \lambda^2$



- $pp \rightarrow ZZjj$ samples
- No $Z \rightarrow ll$ applied
- No fiducial cuts applied
- No SM amplitudes includes
 - only linear and quadratic terms

Sensitivity of QGC operators

$$\mathcal{L}_{EFT} = \mathcal{L}_{SM} + \sum_{j=0,1} \frac{f_{M,j}}{\Lambda^4} \mathcal{O}_{M,j} + \sum_{j=0,1} \frac{f_{S,j}}{\Lambda^4} \mathcal{O}_{S,j} + \sum_{j=0,1} \frac{f_{T,j}}{\Lambda^4} \mathcal{O}_{T,j}$$

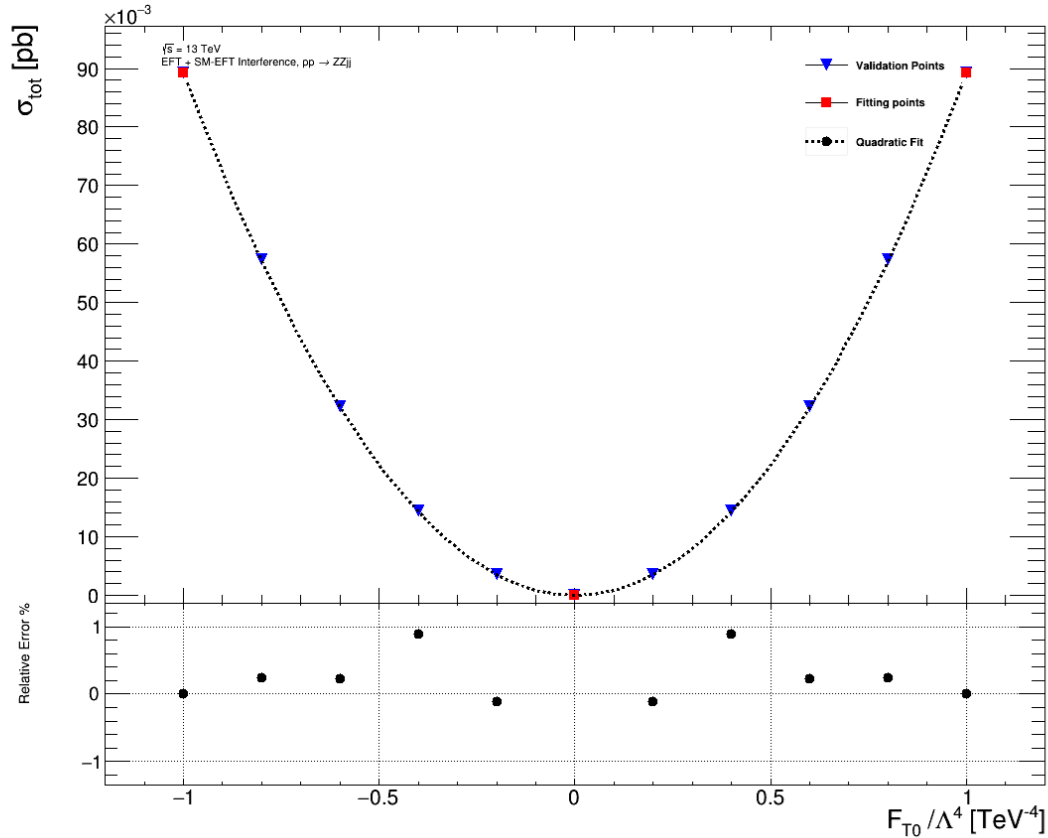


Parameter λ (TeV^{-4})	Quadratic function with SM=0 (pb)
$FT0/\Lambda^4$	$\sigma(\lambda) = 3.725 \cdot 10^{-3} \cdot \lambda + 8.927 \cdot 10^{-2} \cdot \lambda^2$
$FT1/\Lambda^4$	$\sigma(\lambda) = 9.646 \cdot 10^{-4} \cdot \lambda + 5.717 \cdot 10^{-2} \cdot \lambda^2$
$FT2/\Lambda^4$	$\sigma(\lambda) = 1.342 \cdot 10^{-3} \cdot \lambda + 1.377 \cdot 10^{-2} \cdot \lambda^2$
$FT5/\Lambda^4$	$\sigma(\lambda) = 1.180 \cdot 10^{-3} \cdot \lambda + 1.625 \cdot 10^{-2} \cdot \lambda^2$
$FT6/\Lambda^4$	$\sigma(\lambda) = 2.145 \cdot 10^{-4} \cdot \lambda + 7.094 \cdot 10^{-3} \cdot \lambda^2$
$FT7/\Lambda^4$	$\sigma(\lambda) = 3.868 \cdot 10^{-4} \cdot \lambda + 1.495 \cdot 10^{-3} \cdot \lambda^2$
$FT8/\Lambda^4$	$\sigma(\lambda) = 2.265 \cdot 10^{-5} \cdot \lambda + 2.713 \cdot 10^{-2} \cdot \lambda^2$
$FT9/\Lambda^4$	$\sigma(\lambda) = 1.323 \cdot 10^{-5} \cdot \lambda + 5.918 \cdot 10^{-3} \cdot \lambda^2$

- $pp \rightarrow ZZjj$ samples
- No $Z \rightarrow ll$ applied
- No fiducial cuts applied
- No SM amplitudes includes
 - only linear and quadratic terms

$\mathcal{O}_{T,j}$ are the most sensitive operators of the ZZ production.

Limit Setting strategy



To find the quadratic function N_{aQGC} , we fit independent pure QGC and SM-EFT interference samples.

Since for $f_{T_0} = 0$, the event yield is 0, only one extra point is needed.

Total number of expected events:

$$N_{tot} = N_{sm} + N_{aQGC}$$

where $N_{aQGC} = b \cdot f_{Tk} + c \cdot f_{Tk}^2$

and $f_{Tk} = f_{T_0}, f_{T_1}, f_{T_2}, f_{T_5}, f_{T_6}, f_{T_7}, f_{T_8}, f_{T_9}$ the 8-dim operator

Construction of the extended likelihood function with the aQGC parameters

$$L(N_i^{obs}; N_i^{exp}, f_{Tk}) = \prod_{i=1}^{N_{bin}} P(N_i^{obs}, N_i^{exp}) = \prod_{i=1}^{N_{bin}} \frac{e^{-N_i^{exp}} (N_i^{exp})^{N_i^{obs}}}{(N_i^{obs})!}$$

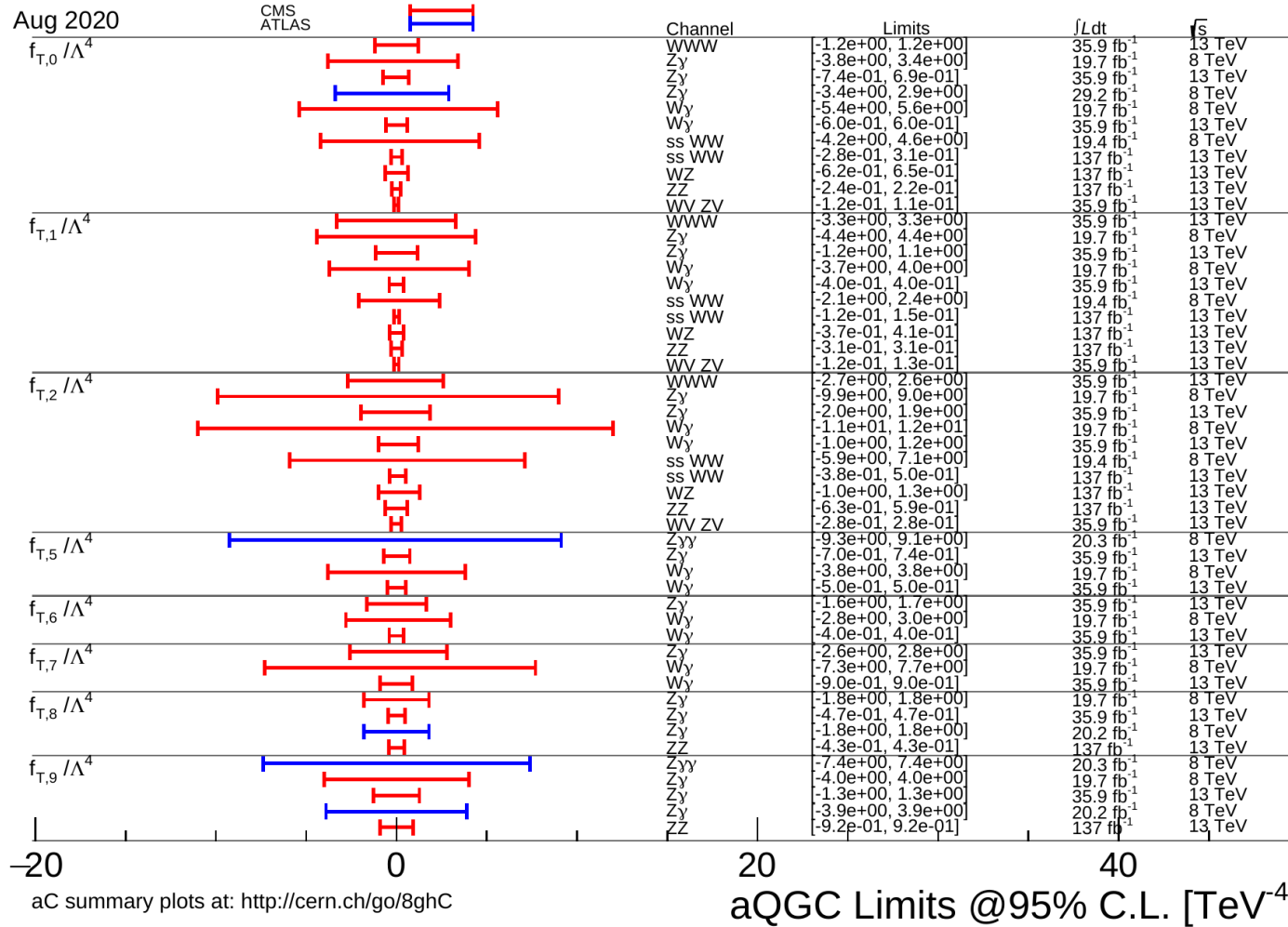
where N_i^{obs} the number of observed events per bin and

$$N_i^{exp} = N_i^{exp}(f_{Tk}) = N_i^{SM} + N_i^{aQGC}$$

the number of expected events per bin

Defining the value of f_{Tk} operator by minimizing $-\log L$

Current limits for f_T operators



Coupling	Exp. lower	Exp. upper	Obs. lower	Obs. upper	Unitarity bound
f_{T0}/Λ^4	-0.37	0.35	-0.24 (-0.26)	0.22 (0.24)	2.4
f_{T1}/Λ^4	-0.49	0.49	-0.31 (-0.34)	0.31 (0.34)	2.6
f_{T2}/Λ^4	-0.98	0.95	-0.63 (-0.69)	0.59 (0.65)	2.5
f_{T8}/Λ^4	-0.68	0.68	-0.43 (-0.47)	0.43 (0.48)	1.8
f_{T9}/Λ^4	-1.5	1.5	-0.92 (-1.02)	0.92 (1.02)	1.8

CMS: Expected and observed lower and upper 95% CL limits on the couplings of the quartic operators T_0 , T_1 and T_2 , as well as the neutral current operators T_8 and T_9 . All coupling parameter limits are in TeV^{-4} , while the unitarity bounds are in TeV .
arXiv:2008.07013

Summary and future plans

- Decomposition method of QGCs works fine : production of independent samples for the linear and quadratic term
 - High BDT importance for the m_{ZZ} : discriminant for future limit setting
 - Sensitivity studies for the selection of QGC operators : $\mathcal{O}_{T,j}$ are far the most sensitive. Limit setting for the operators $f_{T0}, f_{T1}, f_{T2}, f_{T5}, f_{T6}, f_{T7}, f_{T8}, f_{T9}$
-
- ❑ On-going analysis of ATLAS Run-II data and extraction of the differential cross section for the $ZZjj \rightarrow 4lj$ channel
 - ❑ Unitarization: clipping method will be applied during the analysis with a mass cut-off calculated by VBFNLO
 - ❑ Optimization of the binning in m_{ZZ} distribution and use of the high-mass region bins to set constraints on the $\mathcal{O}_{T,j}$ QGC operators

Thank you!

comments?

Backup

Event Generation

- Use of MadGraph5 v2.6.5 @LO with Éboli & Gonzalez-Garcia UFO model for generation of MC samples:

$$pp \rightarrow l^+ l^- l^+ l^- jj$$

and

$$pp \rightarrow ZZjj \rightarrow l^+ l^- l^+ l^- jj$$

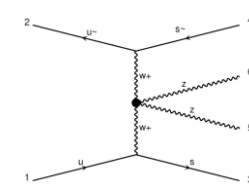
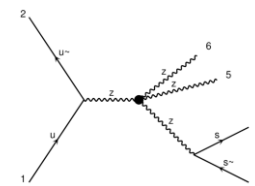
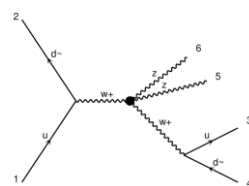
+ Generation of intermediate states including:
 WWZZ, ZZZZ, WWAZ, WWAA, ZZZA, ZZAA,
 ZAAA, AAAA
- Time/CPU consuming

+ Well-defined intermediate state
+ Low cost in terms of time and CPU
- Needs validation ($pp \rightarrow 4ljj$ vs $pp \rightarrow ZZjj \rightarrow 4ljj$)

- Study of $pp \rightarrow 4ljj$ and $pp \rightarrow ZZ \rightarrow 4ljj$ truth information in Les Houches samples and compare the intermediate state bosons for each case in a) Total PS b) Fiducial PS and c) QCD-enriched control region.

Boson(s) in intermediate state	SM (EWK)			Interference			EFT		
	Total	Fiducial	QCD CR	Total	Fiducial	QCD CR	Total	Fiducial	QCD CR
Z	6.13	1.61	2.22	11.08	1.85	5.06	17.00	1.82	11.73
W	0.04	–	0.13	0.04	–	0.15	0.02	–	0.19
H	0.42	–	0.06	–	–	–	–	–	–
ZZ	67.17	98.38	24.76	75.16	98.15	34.60	78.60	98.18	58.07
ZW	1.15	–	3.70	0.90	–	4.12	0.17	–	1.42
ZH	2.64	–	0.96	–	–	–	–	–	–
WH	0.07	–	0.24	–	–	–	–	–	–
ZZZ	10.04	–	31.39	6.85	–	31.04	2.11	–	17.42
ZZW	9.13	–	28.73	5.47	–	24.81	1.27	–	10.45
ZZH	2.27	–	5.61	–	–	–	–	–	–
ZWH	0.44	–	1.38	–	–	–	–	–	–
ZZZH	0.15	–	0.46	–	–	–	–	–	–
ZZWH	0.11	–	0.33	–	–	–	–	–	–
no intermediate state	0.25	0.01	0.03	0.50	–	0.23	0.82	–	0.71

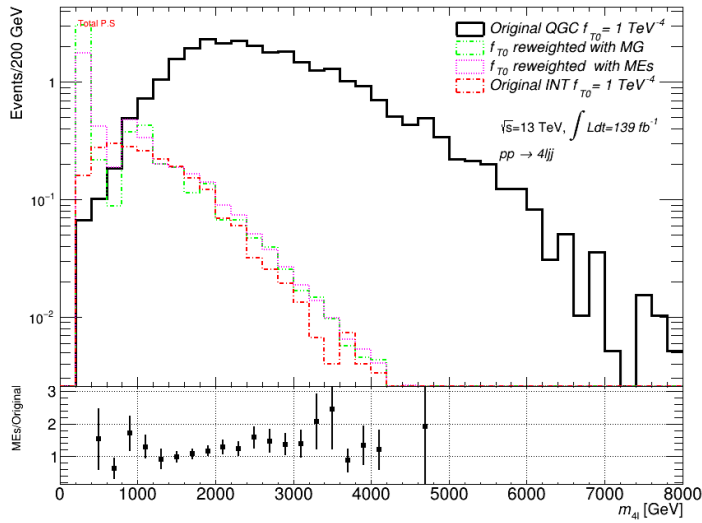
Boson(s) in intermediate state	SM			Interference			EFT		
	Total	Fiducial	QCD CR	Total	Fiducial	QCD CR	Total	Fiducial	QCD CR
ZZ	73.95	100	24.13	88.14	100	42.16	95.8	100	66.68
ZZZ	13.06	–	38.10	8.10	–	39.43	2.64	–	20.92
ZZW	12.04	–	34.86	3.77	–	18.42	1.55	–	12.40
ZZH	0.95	–	2.92	–	–	–	–	–	–



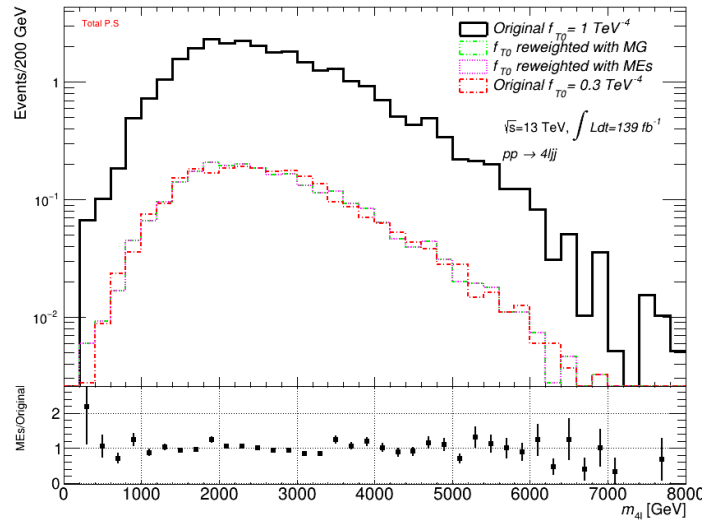
Matrix-Element Re-weighting validation

$$W_{new} = \frac{|M_{new}|^2}{|M_{orig}|^2} \cdot W_{orig}$$

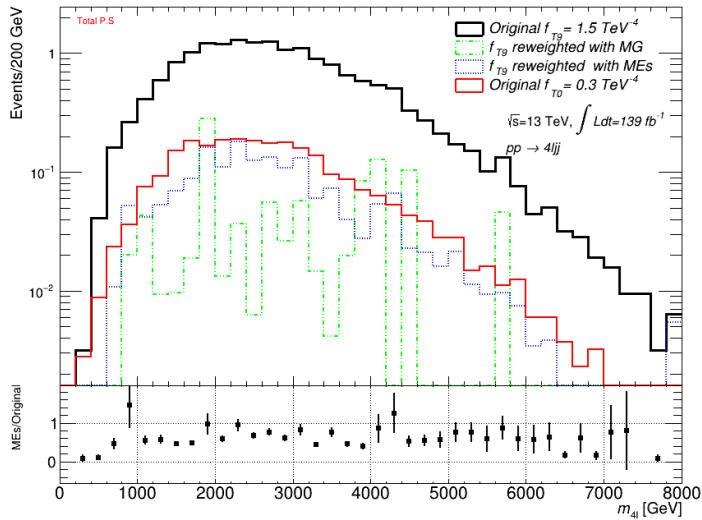
$$\text{where, } W_{orig} = f_1(x_1, \mu_F) \cdot f_2(x_2, \mu_F) \cdot |M_{orig}|^2 \cdot \Omega_{PS}$$



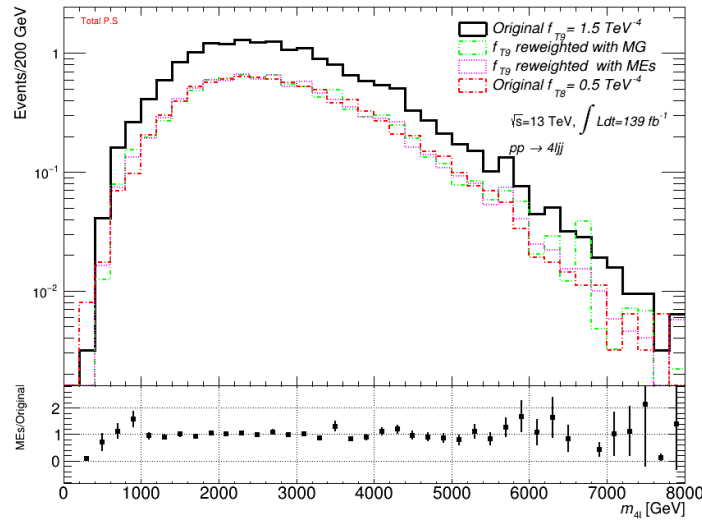
a)



b)



c)



d)

a) Pure QGC sample $f_{T0} = 1$ TeV $^{-4}$ reweighted to SM-EFT Interference with $f_{T0} = 1$ TeV $^{-4}$ (good agreement)

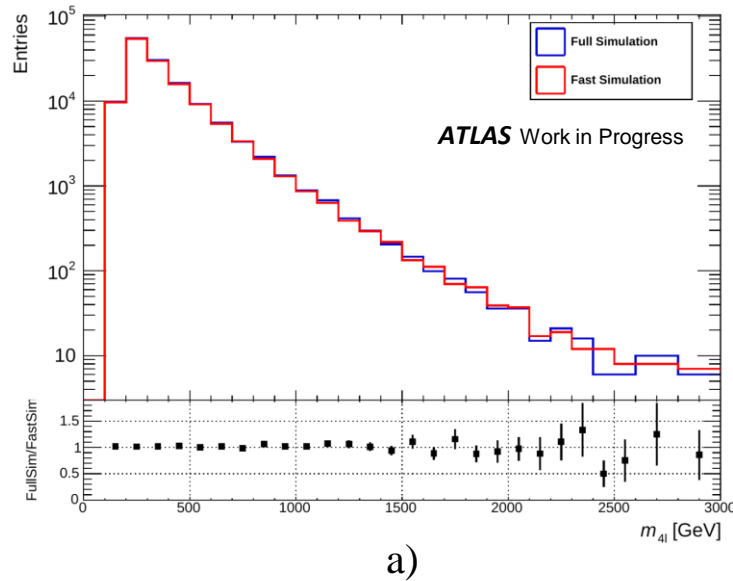
b) Pure QGC sample $f_{T0} = 1$ TeV $^{-4}$ reweighted to pure QGC with $f_{T0} = 0.3$ TeV $^{-4}$ (great agreement)

c) Pure QGC sample $f_{T9} = 1.5$ TeV $^{-4}$ reweighted to pure QGC with $f_{T0} = 0.3$ TeV $^{-4}$ (not possible)

d) Pure QGC sample $f_{T9} = 1.5$ TeV $^{-4}$ reweighted to pure QGC with $f_{T8} = 0.5$ TeV $^{-4}$ (great agreement)

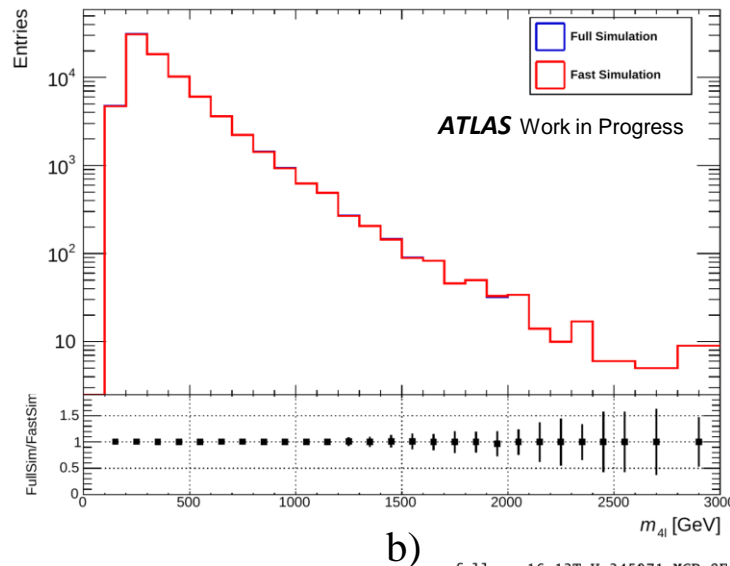
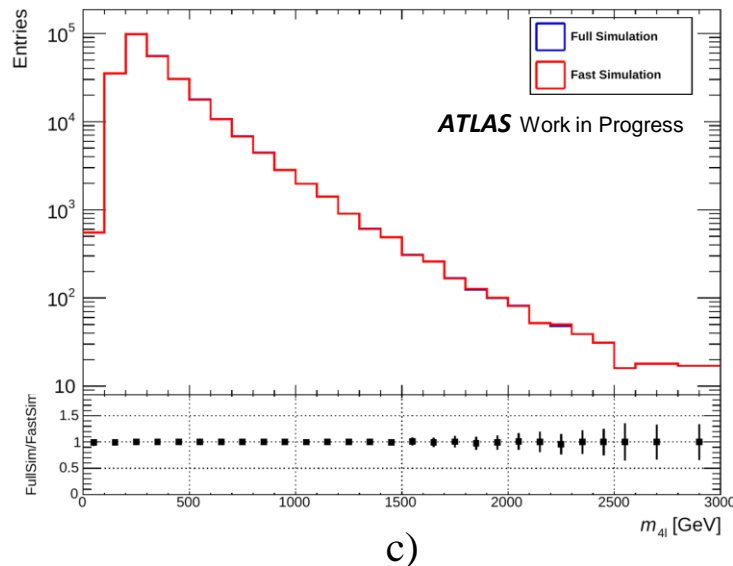
Possibility of re-weighting between values of the same operator or between operators of the same group ($f_{T0}, f_{T1}, f_{T2} - f_{T5}, f_{T6}, f_{T7} - f_{T8}, f_{T9}$)

Full vs Fast Simulation



Comparison between the same truth information reconstructed with ATLAS fast (AFII) and full simulation methods of m_{4l} distributions on a) reconstruction level and on truth level for the b) total and c) fiducial phase space.

Small discrepancy between the two methods. AFII is less time/CPU consuming, providing adequate precision.
Request of VBS aQGC leptonic samples production with AFII simulation: ATLAS PMG - ATLMCPROD-9268

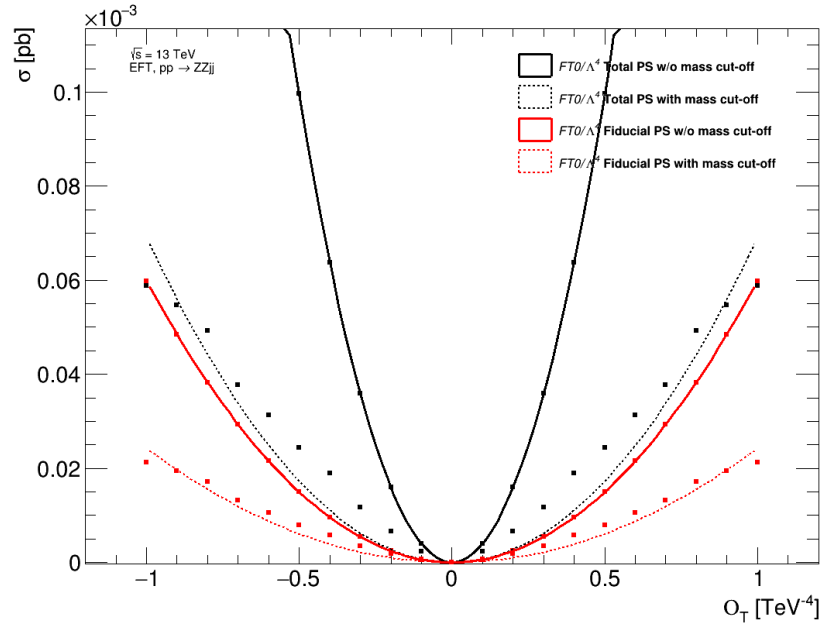


full: mc16_13TeV.345071.MGPy8EvtGen_A14_NNPDF23LO_VBFH125_sbi_4l_m4l1130_EW6.deriv.DAOD_STDM3.e5994_e5984_s3126_r9364_r9315_p3371

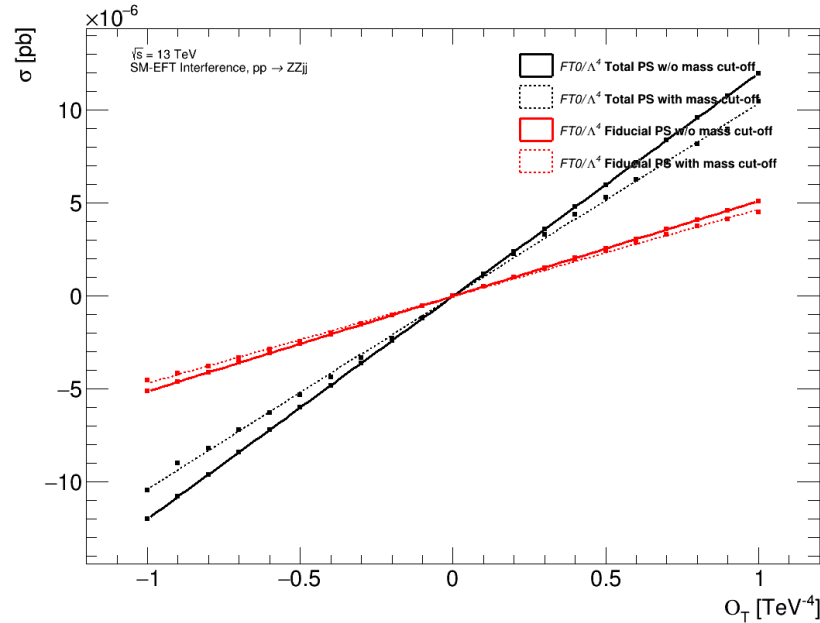
fast: mc16_13TeV.345071.MGPy8EvtGen_A14_NNPDF23LO_VBFH125_sbi_4l_m4l1130_EW6.deriv.DAOD_STDM3.e5994_a875_r9364_r9315_p3598

Unitarity constraints

The contribution of effective operators leads to unitarity violation at high energies.
 ATLAS recommends the generation of un-unitarized MC samples and then apply the “Step-function form-factor” method (aka clipping).



Pure QGC sample with $f_{T0} = [-1,1] TeV$
 in total (black) and fiducial (red) phase space



EFT-SM Interference sample
 with $f_{T0} = [-1,1] TeV$
 in total (black) and fiducial
 (red) phase space

Mass cut-off calculated by
 VBFNLO Form Factor tool

$f_{T0} (TeV^{-4})$	Cut-off bound (TeV)
-1	2
-0.9	2.1
-0.8	2.2
-0.7	2.2
-0.6	2.3
-0.5	2.4
-0.4	2.6
-0.3	2.7
-0.2	3
-0.1	3.6
0	-
0.1	3.6
0.2	3
0.3	2.7
0.4	2.6
0.5	2.4
0.6	2.3
0.7	2.2
0.8	2.2
0.9	2.1
1	2